Open Access

Journal of Energy and Power Technology

LIDSEN Publishing Inc.

Research Article

Enhancing the Wettability of Polyetheretherketone (Peek) Membrane with Ozone for Improving Fuel Cell Performance

Hunter Heineman [1, †], Omran Omar [1, †], Benjamin Rippel [1, †], Ryan Keeley [1, †], Michael Mehan [2, †], Surendra Gupta [3, †], Gerald A. Takacs [1, †, *]

1. School of Chemistry and Materials Science, Rochester Institute of Technology, Rochester, NY, USA; E-Mails: hdh3020@g.rit.edu; omranoma@buffalo.edu; bwr9457@g.rit.edu; rpk8784@g.rit.edu; gatsch@rit.edu
2. Xerox Analytical Services, Xerox Corporation, Webster, NY, USA; E-Mail: Michael.Mehan@xerox.com
3. Department of Mechanical Engineering, Rochester Institute of Technology, Rochester, NY, USA; E-Mail: skgeme@rit.edu

† These authors contributed equally to this work.

* **Correspondence:** Gerald A. Takacs; E-Mail: gatsch@rit.edu

Academic Editors: Giosue Giacoppo and Orazio Barbera

Special Issue: Development, Design, Test, and Modeling of Low Temperature Fuel Cells

Journal of Energy and Power Technology
2022, volume 4, issue 4
doi:10.21926/jept.2204040

Received: August 21, 2022
Accepted: November 24, 2022
Published: December 06, 2022

Abstract

Ozone was reacted with the aromatic membrane polyetheretherketone (PEEK) to form oxidized functional groups on the surface to enhance the attraction and transport of protons in fuel cells. Ozonation of unsaturated C-C sp^2 bonds in PEEK formed a primary ozonide which dissociated to primarily produce O=C-O/O=C-OH moieties, and the root mean squared roughness factor (R_q) decreased from 7.4 nm, for the untreated sample, down to 3.1 nm. The oxidation of the surface and decrease in surface roughness made the surface increase in hydrophilicity as observed by the decrease in the water contact angle (CA) from 80.3° for untreated PEEK down to 21.7°. Washing the treated surface with solvent decreased the O at %

on the surface indicating the formation of a weak boundary layer because of bond breakage during the decomposition of the ozonide.

Keywords
Fuel cells; polyetheretherketone; ozone

1. Introduction

Renewable energy sources, such as, solar, wind, biomass, geothermal, and fuel cells, are providing important solutions to dependence on fossil fuels and reduction in climate change [1-3]. In a proton exchange membrane fuel cell (PEMFC), a polymer membrane is placed between two electrodes to form a membrane electrode assembly (MEA), which with hydrogen as the fuel, produces only water and heat as the by-products making the fuel cell an environmentally friendly technology [4-7].

In the 1960s, Dupont developed the first ion exchange membrane, Nafion®, consisting of a perfluorinated backbone having sulfonic acid groups, $-SO_3H$, for high proton conductivity which depended on its water content and dehydrated at temperatures higher than 90°C [7, 8]. Since higher temperatures ($T \geq 100$°C) are often used in PEMFCs, modification of Nafion membranes have been studied, as well as, the development of novel conductive membranes consisting of the inorganic proton conductor, calcium phosphate, and ionic liquids supported on polytetrafluoroethylene [8].

For high temperature PEMFCs, phosphoric acid doped polybenzimidazole (PBI) membrane, is frequently used for proton conductivity via hydrogen bonding between the phosphoric acid and the nitrogen-containing groups in PBI [9-13]. However, at this high temperature, there is loss of H_3PO_4 decreasing the performance of the fuel cell [14-17]. Therefore, to increase wettability and proton conductivity, surface oxidation of the aromatic groups in PBI were studied with ozone [18], O atoms [19], UV photo-oxidation [20], and vacuum UV photo-oxidation [21]. In addition, the performance of a phosphoric acid fuel cell with n-hexadecane fuel has shown promise for petroleum diesel or biodiesel fuels [22].

The high performance semicrystalline thermoplastic aromatic polymer, polyetheretherketone (PEEK) (Figure 1) has good mechanical properties, high thermal glass transition (143°C) and melting temperatures (343°C), as well as, chemical stability [23] resulting in many applications including the aerospace industry [24-26] and sterilization of water [27], where reaction with ozone may occur, as well as, in fuel cells [28]. However, PEEK lacks a sufficient level of proton conductivity and durability for fuel cells thus requiring modification [28], such as, sulfonation of PEEK to increase proton conductivity and higher stability [29].

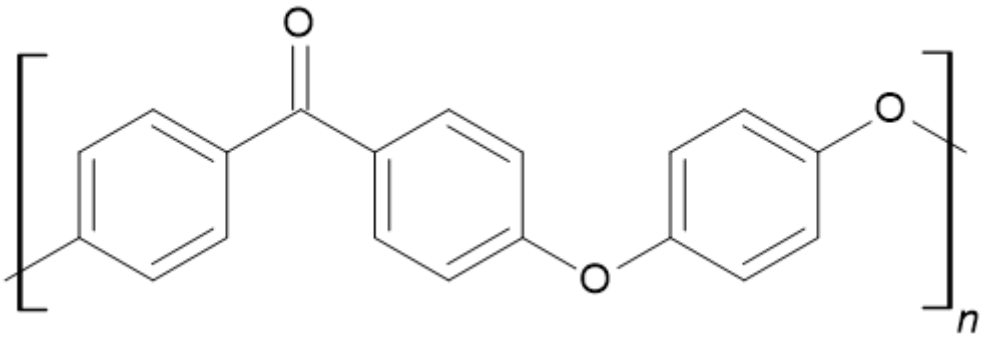

Figure 1 Molecular structure of polyetheretherketone (PEEK).

Interfacial properties of the fuel cell membrane are key to operation of the MEAs [30] and to attract protons the polar groups on the polymer backbone must be maximized [31]. Despite all of its benefits, the non-polar aromatic backbone of PEEK exhibits hydrophobic characteristics which limit adhesion and transport of protons [25, 32, 33]. Therefore, to decrease hydrophobicity, this research investigated oxidation of PEEK with ozone and measured surface changes in chemistry, surface roughness, and hydrophilicity with treatment time using X-ray Photo-electron Spectroscopy (XPS), Atomic Force Microscopy (AFM), and water contact angle (CA*)*, respectively.

2. Materials and Methods

2.1 Materials

Aldrich (GF77849881-5EA) 0.2 mm thick PEEK film was used which had glossy and rough sides. XPS detected small amounts of Si contamination in the silane/siloxane region of the Si 2p spectra. Therefore, the PEEK samples were cleaned by four procedures: abrading, low energy sputtering, and washing with isopropyl alcohol or hexane. Since hexane removed all the Si and the XPS atomic percentages (at %) agreed within experimental error of the theoretical value for the structure of PEEK, the glossy side of PEEK cleaned with hexane was treated.

2.2 Production of Ozone

This study was conducted similar to the reaction of ozone with polybenzimidazole (PBI) [18] where oxygen with a flow rate of 2.5 l/h was fed into an Enaly Ozone Generator model 1000BT-12 (Shanghai, China), which contains a corona discharge tube, to convert about 6 ± 2% of the volume of oxygen into ozone. The ozone/oxygen mixture was then flowed over the sample in a quartz cylindrical cell with the exiting gas passed through a solution of KI to convert the remaining ozone to oxygen before emission into the vacuum hood.

2.3 X-ray Photoelectron Spectroscopy (XPS)

Physical Electronics Versaprobe II 5000 XPS analyzed the top 2–5 nm of a rectangular region of about 1400 µm by 600 µm of the sample's surface with a take-off angle of 45°. The quantitative analyses are precise to within 5 and 10% relative for major and minor constituents, respectively.

The high resolution C 1s and O 1s spectra were normalized to the peak intensities at the main hydrocarbon and C-O peaks, respectively. Initially, curve-fitting was done by subtracting the control spectrum from that of the treated sample to determine the number of peaks, their binding energies, and peak widths. The peaks were then used to curve-fit the total treated spectrum. Any missing peaks, such as weak energy loss peaks, were then added to achieve a good chi square fit. A materials balance was calculated to test if the results of the curve fitting agreed with the concentrations as determined from the quantitative analyses.

2.4 Atomic Force Microscopy (AFM)

Surface roughness was measured using a Bruker DI-3000 AFM in the tapping mode. For each specimen, a 15 μm × 15 μm image was obtained with the same Olympus OTESPA tip.

2.5 Contact Angle (CA) Goniometry

A Ramé-Hart model 250-F1 Standard Contact Angle Goniometer was used to determine the water CA. A micropipette was used to deposit a 10 μL deionized water droplet on the surface. As soon as the water droplet was placed on the film, a picture was captured by the U1 Series Camera. The left side and the right side contact angles were measured by the functioning DROPimage contact angle (CA) program. The standard deviation of the measurements was about ±2.5°.

This research did not involve any human, animal, plant or subjects requiring an ethics committee or institutional review board approval.

3. Results

3.1 XPS Quantitative Analyses

XPS detected only C and O on four hexane cleaned and untreated samples with the average O at % being 13.7 ± 0.2 in good agreement with the 13.6 at % O in the molecular structure of PEEK (Figure 1).

Three separate sets of hexane cleaned PEEK samples were treated with ozone for 15, 30, 45 and 60 min resulting in a saturation level of 22.3 ± 0.2 at % O after ca. 15 min of treatment.

3.2 XPS Chemical State Analysis

An example of the overlapped C 1s spectra for the control and ozone-treated PEEK samples are displayed in Figure 2 with the curve-fitting results in Table 1 showing primarily a decrease in C-C aromatic ring bonding and formation of the O=C-O/O=C-OH moieties, and a small increase in the C-O and C=O functional groups.

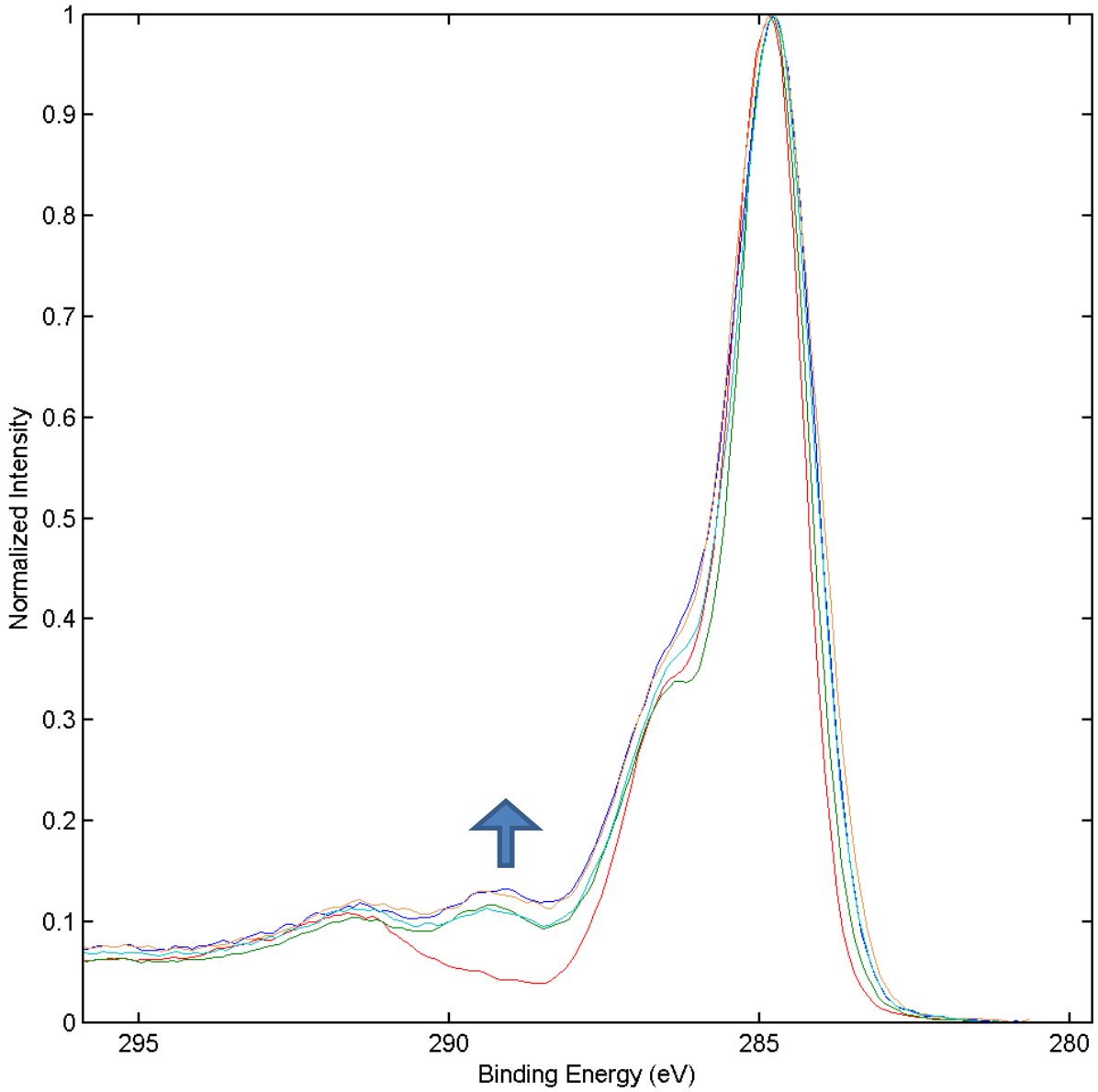

Figure 2 C 1s spectra for control and ozone-treated PEEK samples with the arrow indicating increasing treatment time for 0 (red), 15 (blue), 30 (green), 45 (orange) and 60 (light blue) min.

Table 1 Assignments [34] and % areas for the C 1s peaks in Figure 2 as determined by curve-fitting.

Binding Energy (eV)	Species	Treatment Time (min)				
		0	15	30	45	60
284.7	C-C, aromatic ring	70.0	66.0	66.9	66.2	66.9
286.3	C-O	17.9	18.9	18.0	18.6	18.7
287.1	C=O	4.9	5.7	5.8	6.8	5.7
289.0	O=C-O, O=C-OH	0.0	4.5	4.5	4.8	4.7
291.6	Energy Loss Peak	7.2	4.9	4.8	3.6	4.0

For the same samples, the overlapped O 1s spectra are shown in Figure 3 with the curve-fitting results in Table 2 confirming the substantial increase in the presence of the O=C-O/O=C-OH moieties.

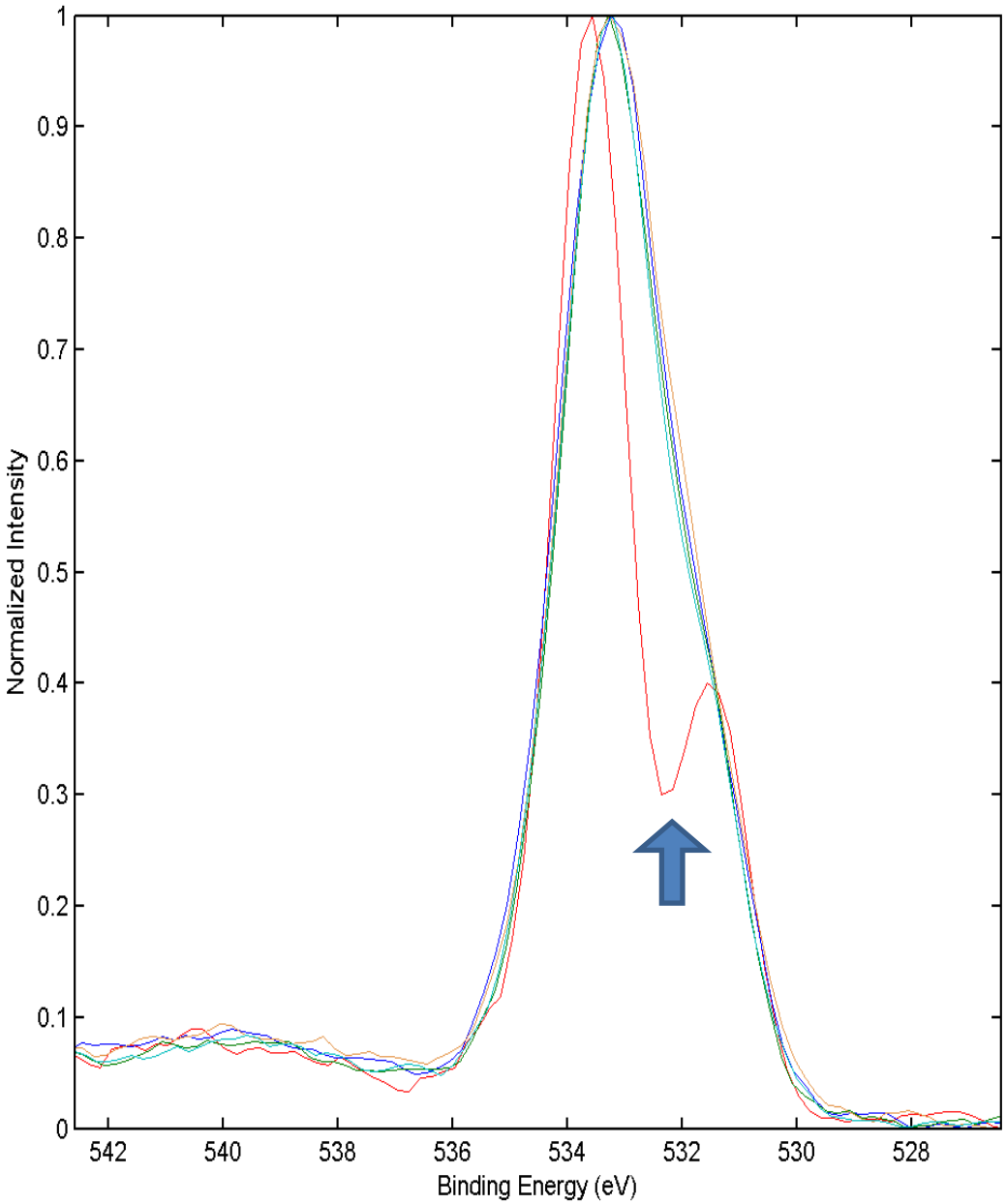

Figure 3 O 1s spectra for control and ozone-treated PEEK samples with the arrow indicates increasing treatment time for 0 (red), 15 (blue), 30 (green), 45 (orange), and 60 (light blue) min.

Table 2 Assignments [34] and % areas for the O 1s peaks in Figure 3 as determined by curve-fitting.

Binding Energy (eV)	Species	Treatment Time (min)				
		0	15	30	45	60
531.4	O=C	28.2	16.6	16.7	19.2	17.0
532.2	O=C-O, O=C-OH	0.0	36.2	35.9	34.4	38.8
533.6	(ring) C-O-C (ring)	71.8	47.2	47.4	46.4	44.2

3.3 Surface Topography for PEEK Treated with Ozone

AFM measurements of the treated surface showed a decrease in the root mean squared roughness factor (R_q) from 7.4 nm, for the untreated sample, down to 3.1 nm after 60 min of treatment (Figure 4).

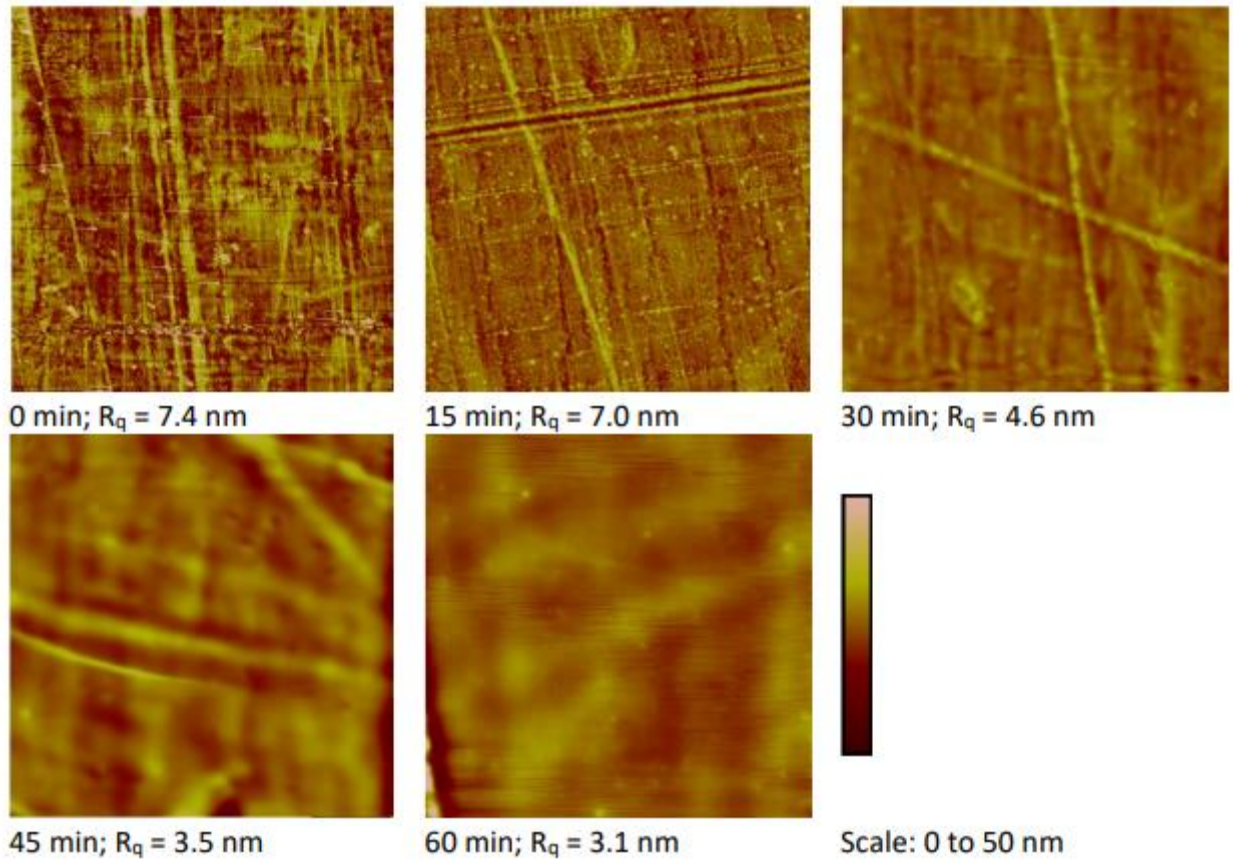

Figure 4 AFM surface topographic images (15 μ × 15 μ) showing the root mean squared roughness factors (Rq) in nms after treatment for 0, 15, 30, 45, and 60 min.

3.4 Water Contact Angle (CA) Measurements

As shown in Figure 5, treatment of PEEK with ozone made the surface more hydrophilic with treatment time.

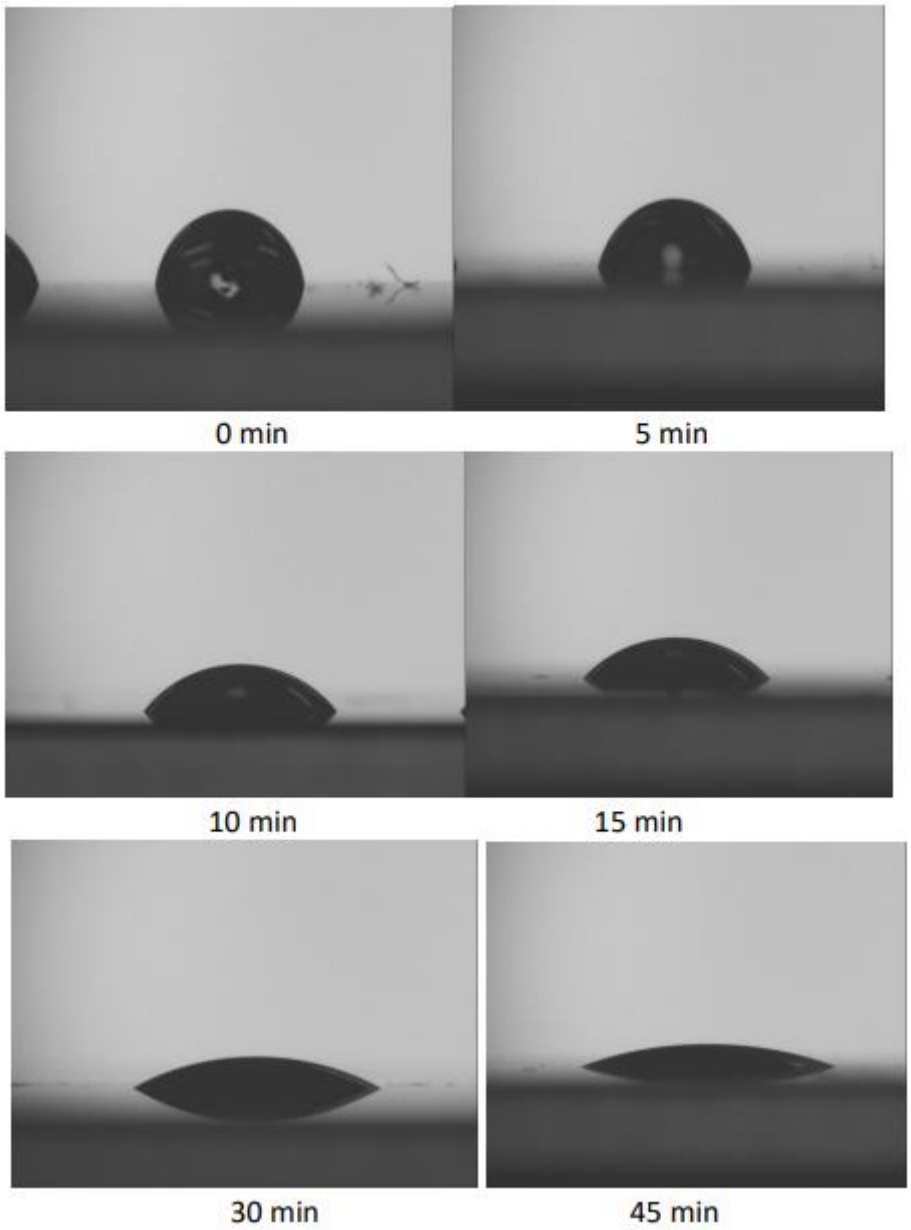

Figure 5 Images of water droplet on PEEK surfaces as a function of treatment time with ozone.

On average, the CA decreased from 80.3° for the control sample down to 21.7° after 45 min of treatment time (Figure 6). However, as shown in Figure 6, washing the treated samples with ethanol increased the CA back up to ca. 55°.

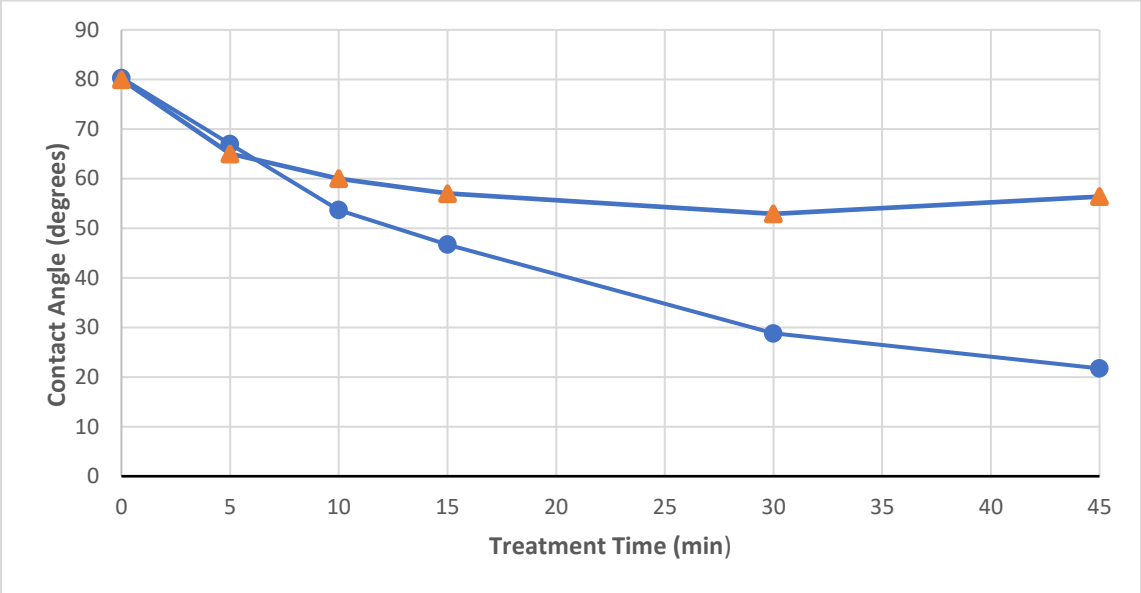

Figure 6 Water contact angle as a function of treatment time for ozone reacting with PEEK (•) and then washed with ethanol after treatment (▲).

4. Discussion

Little research was done previously on ozone-gas treatment of PEEK. In this study, cleaning of four samples of untreated PEEK with hexane gave an O at % of 13.7 ± 0.2 in good agreement with the theoretical value of 13.6 at % in the molecular structure of PEEK (Figure 1). When a PEEK board was machined to obtain discs which were sandblasted with alumina particles and then treated with gaseous ozone the O at % reported was 19.05 ± 0.33 for a bare sample [35]. In this study, the O at % for treated PEEK samples increased up to a saturation level of 22.3 ± 0.2 at % compared to 34.88 ± 0.93 at % [35] which probably used higher concentrations of ozone. The O 1s XPS spectra (Figure 3) showed the formation of a new peak at 532.2 eV corresponding to the ester/carboxylic acid, O=C-O/O=C-OH, functional groups which contains the O-H bond that was reported to react with phosphoryl chloride in the presence of trimethylamine to prepare phosphate-modified PEEK [35]. UV/ozone photo-oxidation of PEEK also reported the development of the C 1s XPS peak due to the formation of the ester/carboxylic acid groups [36].

Since the reaction of ozone with ethers in organic solutions indicate the attachment of ozone to α-hydrogen near the ether group [37], Figure 7 shows ozonation of the unsaturated C-C sp^2 bond closest to the ether group in PEEK to form a primary ozonide [38] similar to the reaction of ozone with the fuel cell membrane polybenzimdazole (PBI) [18]. Figure 7 displays the possible decomposition steps marked “a” and “b” in addition to breakage of the “c” bond. Breakage of the “b” bond forms a compound containing the ester/carboxylic moieties, which is detected in this study (Table 1 and Table 2), and a criegee intemediate that may also produce an ester group with the release of CO_2 [38]. While step “a” would form an C=O containing aldehyde and an oxygenated criegree intermediate that could produce a O-(C=O)-O containing product which was not detected in this study (Table 2). Thus, the preferred pathway of decomposition appears to be step “b” consistent with the decomposition of PBI [18] where nitrogen-containing, and not oxygen-containing, groups are in the PBI stucture.

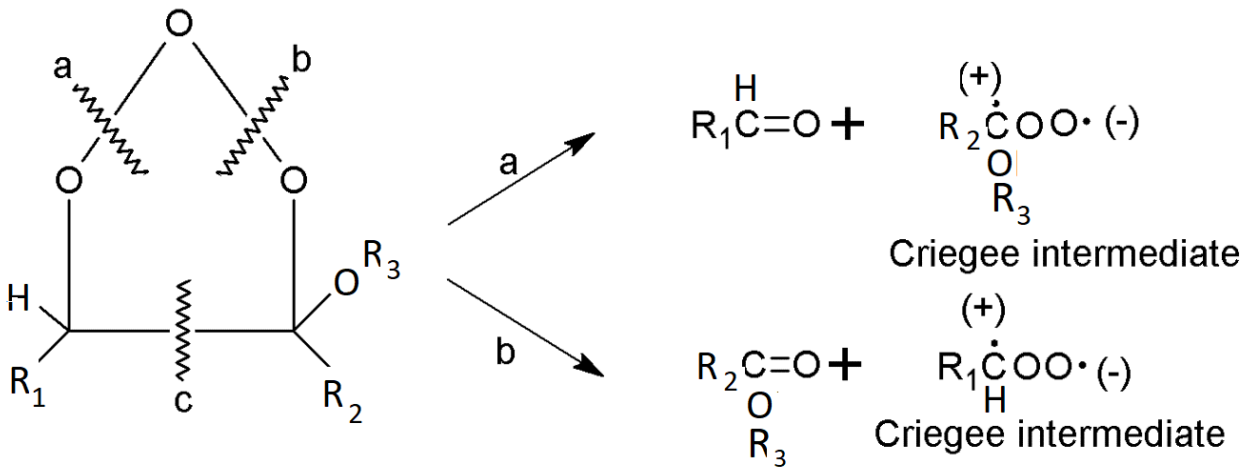

Figure 7 Decomposition of the primary ozonide of PEEK [38].

The increase in oxidation of the surface and decrease in surface roughness both contribute to the decrease in CA and increase in hydrophilicity relative to untreated PEEK. Breakage of the bonds with ozonization leads to the formation of a weak boundary layer which is washed away with solvent increasing the CA (Figure 6).

5. Conclusions

Hexane cleaning of untreated fuel cell membrane PEEK gave an O at % of 13.7 ± 0.2 in good agreement with 13.6 at % in its molecular structure. Gas phase treatment of PEEK with ozone increased the O concentration up to a saturation level of 22.3 ± 0.2 at %. Water contact angle measurements showed that the surface became more hydrophilic due to the formation of O=C-O/O=C-OH moieties and a decrease in surface roughness. Washing the treated PEEK samples decreased the O at % indicating the formation of a weak boundary layer due to breakage of bonds during the decomposition of the primary ozonide. Oxidation of PEEK with ozone added polar functional groups to the surface which should help attract protons in fuel cells.

Acknowledgments

The authors gratefully acknowledge Nathan Eddingsaas for use of the ozone generator and Tom Allston for help with the figures.

Author Contributions

Hunter Heineman, Omran Omar, Benjamin Rippel, and Ryan Keeley did the experiments and CA measurements. Michael Mehan and Surendra Gupta performed the XPS and AFM analyses, respectively. Gerald Takacs initiated the research, supervised the experiments, and wrote the manuscript.

Funding

Support for this research was provided by Xerox Analytical Services, Xerox Corporation, Webster, NY, USA.

Competing Interests

The authors have declared that no competing interests exist.

References

1. Al-Anazi A, Wilberforce T, Khatib FN, Vichare P, Olabi AG. Performance evaluation of an air breathing Polymer Electrolyte Membrane (PEM) fuel cell in harsh environments-a case study under Saudi Arabia's ambient condition. Int J Hydrog Energy. 2021; 46: 23463-23479.
2. Tawalbeh M, Al-Othman A, Abdelwahab N, Alami AH, Olabi AG. Recent developments in pressure retarded osmosis for desalination and power generation. Renew Sustain Energy Rev. 2021; 138: 110492.
3. Tawalbeh M, Al-Othman A, Singh K, Douba I, Kabakebji D, Alkasrawi M. Microbial desalination cells for water purification and power generation: A critical review. Energy. 2020; 209; 118493.
4. Press RJ, Santhanam KSV, Miri MJ, Bailey AV, Takacs GA. Introduction to hydrogen technology. Hoboken, New Jersey: John Wiley & Sons Inc.; 2009.
5. Bailey A, Andrews L, Khot A, Rubin L, Young J, Allston TD, et al. Hydrogen storage experiments for an undergraduate laboratory course-clean energy: Hydrogen/fuel cells. J Chem Educ. 2015; 92: 688-692.
6. Santhanam KSV, Takacs GA, Miri MJ, Bailey AV, Allston TD, Press RJ. Clean energy: Hydrogen/fuel cells laboratory manual. Singapore: World Scientific Publishing Co.; 2016.
7. Santhanam KSV, Press RJ, Miri MJ, Bailey AV, Takacs GA. Introduction to hydrogen technology. 2nd ed. Hoboken, New Jersey: John Wiley & Sons, Inc.; 2018.
8. Ka'ki A, Alraeesi A, Al-Othman A, Tawalbeh M. Proton conduction of novel calcium phosphate nanocomposite membranes for high temperature PEM fuel cells applications. Int J Hydrog Energy. 2021; 46: 30641-30657.
9. Haider R, Wen Y, Ma ZF, Wilkinson DP, Zhang L, Yuan X, et al. High temperature proton exchange membrane fuel cells: Progress in advanced materials and key technologies. Chem Soc Rev. 2021; 50: 1138-1187.
10. Li Q, Jensen JO, Savinell RF, Bjerrum NJ. High temperature proton exchange membranes based on polybenzimidazoles for fuel cells. Prog Polym Sci. 2009; 34: 449-477.
11. Wainright JS, Wang JT, Weng D, Savinell RF, Litt M. Acid-doped polybenzimidazoles: A new polymer electrolyte. J Electrochem Soc. 1995; 142: L121-L123.
12. Quartarone E, Mustarelli P. Polymer fuel cells based on polybenzimidazole/H_3PO_4. Energy Environ Sci. 2012; 5: 6436-6444.
13. Kondratenko MS, Gallyamov MO, Khokhlov AR. Performance of high temperature fuel cells with different types of PBI membranes as analysed by impedance spectroscopy. Int J Hydrog Energy. 2012; 37: 2596-2602.
14. Seel DC, Benicewicz BC, Xiao L, Schmidt TJ. High-temperature polybenzimidazole-based membranes. In: Handbook of fuel cells–fundamentals, technology and applications. Chichester, UK: John Wiley & Sons, Ltd.; 2009. pp. 300-313.
15. Yu S, Xiao L, Benicewicz BC. Durability studies of PBI-based high temperature PEMFCs. Fuel Cells. 2008; 8: 165-174.

16. Kim JR, Yi JS, Song TW. Investigation of degradation mechanisms of a high-temperature polymer-electrolyte-membrane fuel cell stack by electrochemical impedance spectroscopy. J Power Sources. 2012; 220: 54-64.
17. Jakobsen MTD, Jensen JO, Cleemann LN, Li Q. Durability issues and status of PBI-based fuel cells. In: High temperature polymer electrolyte membrane fuel cells. Cham, Switzerland: Springer International Publishing; 2016. pp. 487-509.
18. Omar O, Ha B, Vega K, Fleischer A, Moon H, Shertok J, et al. Reaction of ozone with polybenzimidazole (PBI). Ozone Sci Eng. 2018; 40: 392-398.
19. Vega K, Cocca M, Le H, Toro M, Garcia A, Fleischer A, Bailey A, et al. Enhancing the wettability of polybenzimidazole (PBI) to improve fuel cell performance. In: Advances in contact angle, wettability and adhesion. Scrivener Publishing LLC; 2019. pp. 179-193.
20. Shedden D, Atkinson KM, Cisse I, Lutondo S, Roundtree T, Teixeira M, et al. UV photo-oxidation of polybenzimidazole (PBI). Technologies. 2020; 8: 52.
21. Kovach T, Boyd S, Garcia A, Fleischer A, Vega K, Hilfiker R, et al. Surface modification of polybenzimidazole (PBI) with microwave generated vacuum ultraviolet (VUV) photo-oxidation. Curr Microw Chem. 2022; 9: 10-17.
22. Zhu Y, Robinson T, Al-Othman A, Tremblay AY, Ternan M. n-Hexadecane fuel for phosphoric acid direct hydrocarbon fuel cell. J Fuels. 2015; 2015: 748679.
23. Kurtz SM, Devine JN. PEEK biomaterials in trauma, orthopedic, and spinal implants. Biomaterials. 2007; 28: 4845-4869.
24. Kleiman J. Surface modification of polymers used in low earth orbit space environment. In: metallized plastics 5 & 6: Fundamental and applied aspects. London: CRC Press; 1998. pp. 331-351.
25. Arikan E, Holtmannspötter J, Hofmann T, Gudladt HJ. Vacuum-UV of polyetheretherketone (PEEK) as a surface pre-treatment for structural adhesive bonding. J Adhes. 2020; 96: 917-944.
26. Yousaf A, Farrukh A, Oluz Z, Tuncel E, Duran H, Doğan SY, et al. UV-light assisted single step route to functional PEEK surfaces. React Funct Polym. 2014; 83: 70-75.
27. Ohmi T, Isagawa T, Imaoka T, Sugiyama L. Ozone decomposition in ultrapure water and continuous ozone sterilization for a semiconductor ultrapure water system. J Electrochem Soc. 1992; 139: 3336.
28. Raja Rafidah RR, Rashmi W, Khalid M, Wong WY, Priyanka J. Recent progress in the development of aromatic polymer-based proton exchange membranes for fuel cell applications. Polymers. 2020; 12: 1061.
29. Nimir W, Al-Othman A, Tawalbeh M, Makky AA, Ali A, Karimi-Maleh H, et al. Approaches towards the development of heteropolyacid-based high temperature membranes for PEM fuel cells. Int J Hydrog Energy. 2021. doi: 10.1016/j.ijhydene.2021.11.174.
30. Gubler L, Scherer GG. A proton-conducting polymer membrane as solid electrolyte – Function and required properties. Adv Polym Sci. 2008; 215: 1-14.
31. Chandan A, Hattenberger M, El-Kharouf A, Du S, Dhir A, Self V, et al. High temperature (HT) polymer electrolyte membrane fuel cells (PEMFC) – A review. J Power Sources. 2013; 231: 264-278.
32. Yousaf A, Farrukh A, Oluz Z, Tuncel E, Duran H, Doğan SY, et al. UV-light assisted single step route to functional PEEK surfaces. React Funct Polym. 2014; 83: 70-75.

33. Verma S, Sharma N, Kango S, Sharma S. Developments of PEEK (Polyetheretherketone) as a biomedical material: A focused review. Eur Polym J. 2021; 147: 110295.
34. Beamson G, Briggs D. High resolution XPS of organic polymers. Sussex: John Wiley & Sons, Inc.; 1992.
35. Sunarso, Tsuchiya A, Toita R, Tsuru K, Ishikawa K. Enhanced osseointegration capability of poly (ether ether ketone) via combined phosphate and calcium surface-functionalization. Int J Mol Sci. 2019; 21: 198.
36. Mathieson I, Bradley RH. Effects of ultra violet/ozone oxidation on the surface chemistry of polymer films. Key Eng Mater. 1995; 99: 185-192.
37. Rakovsky S, Anachkov M, Belitskii M, Zaikov G. Kinetics and mechanism of the ozone reaction with alcohols, ketones, ethers and hydroxybenzenes. Chem Chem Technol. 2016; 10: 531-552.
38. Finlayson-Pitts BJ, Pitts Jr JN. Chemistry of the upper and lower atmosphere. New York: Academic Press; 2000.